High Resolution Microscopy of PMDA–ODA Poly(imide) Single Crystals

Jaime R. Ojeda† and David C. Martin*

Materials Science and Engineering and the Macromolecular Science and Engineering Center, University of Michigan, College of Engineering, 2022 H. H. Dow Building, 2300 Hayward Street, Ann Arbor, Michigan 48109-2136

Received May 26, 1993; Revised Manuscript Received August 23, 1993•

ABSTRACT: Single crystals of the poly(imide PMDA–ODA were grown from a 1.4% by weight solution of the precursor poly(amic acid) in 1-methyl-2-pyrrolidinone (NMP) solvent. The morphology of the crystals was examined by high resolution electron (HREM) and atomic force microscopies (AFM). The crystals formed spherulitic bundles of well-defined lamellae similar to that typically observed in semicrystalline polymers. The crystallographic growth direction was found to be [010] in all cases. The nucleation and growth patterns of these crystals permitted imaging of the lateral ((100) 0.6-nm and (010) 0.4-nm) packing directions as well as that along the chain axis. High contrast 1.6-nm (002) lattice fringes seen within the polymer lamellae provided direct evidence of the crystalline perfection and for screw dislocation mediated crystal growth and lamellar branching. The lamellar crystal thickness was found to be 10.2 ± 0.5 nm, corresponding to six PMDA–ODA repeat units along the (c) chain axis. Evidence from [001] zone HREM images and electron diffraction patterns indicated that the crystallographic angle (γ) fluctuated locally from 81 to 99°. This was consistent with molecular simulations indicating that the crystal energy of PMDA–ODA was relatively insensitive to fluctuations over a similar range of angles. The theoretical simulations also indicate that fluctuations in γ should be accompanied by simultaneous variations in the molecular setting angle θ.

I. Introduction and Background

Pyromellitic dianhydride–oxydianiline (PMDA–ODA) poly(imide) has been used in a wide variety of applications because of its mechanical properties, low dielectric constant, and thermal stability. PMDA–ODA poly(amic acid) (PAA), the tractable precursor polymer to PMDA–ODA poly(imide) (PI), is prepared by a condensation reaction from the dianhydride (PMDA) and the diamine (ODA). The conversion of PMDA–ODA PAA to PI (Figure 1) involves local conformational rearrangements along the precursor PAA chain. Since the imide is insoluable in most solvents the precursor polymer solution is usually cast or spin-coated onto substrates.

Information about the microstructural organization of PMDA–ODA is important for interpreting its macroscopic properties. X-ray scattering studies of PMDA–ODA fibers and films have revealed a morphology which is a strong function of the specific processing route employed.[1–7] Wide angle X-ray scattering (WAXS) studies[5,6] have shown that the PMDA–ODA molecules obtain a high degree of molecular organization when orientation is induced by the presence of a substrate or by mechanical deformation. Grazing incidence X-ray scattering (GIXS) studies[5] on PMDA–ODA films cured on silicon substrates have revealed highly crystalline ordering near the free surface while the bulk of the film is more disordered.[1,3]

This investigation was undertaken to discern the structural organization in PMDA–ODA lamellar single crystals grown from dilute solution. We anticipated that, by studying PMDA–ODA lamellar single crystals, information about the nature and perfection of local molecular order in PMDA–ODA could be obtained. This information provides new insight about the organization of crystalline PMDA–ODA and makes it possible to compare this morphology with that found in commercially available films and films cured near surfaces.

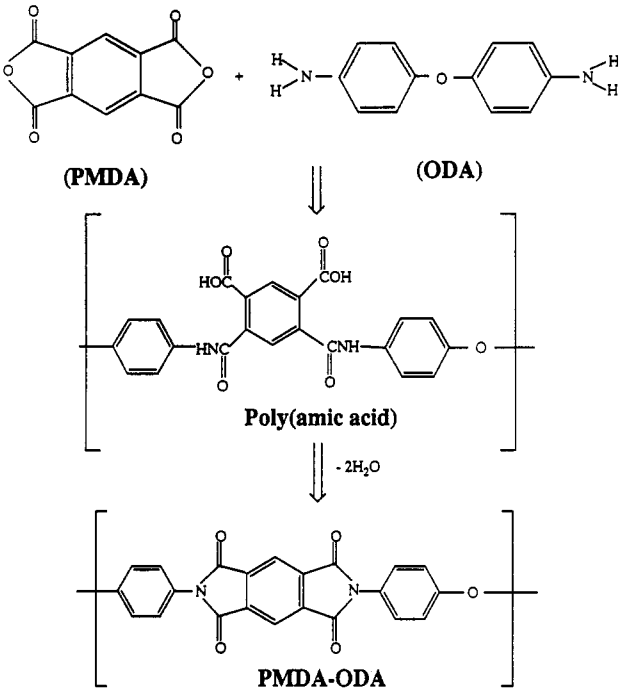

Figure 1. Synthesis of PMDA–ODA involving a condensation reaction between pyromellitic dianhydride (PMDA) and oxydianiline (ODA) to make a poly(amic acid). The poly(amic acid) liberates two molecules of water per repeat unit to make the final PMDA–ODA poly(imide).

PMDA–ODA lamellar single crystals have been studied previously by transmission electron microscopy (TEM) and electron diffraction (ED) by Lebedev.[8] As is typical for crystalline polymers, the molecular chain direction was found to be oriented perpendicular to the lamellar surface. The lamellae were determined to be 5–6 nm thick. The apparent folding of the PMDA–ODA chain was attributed to unconverted PAA segments, with the argument made that three of every four chemical repeats would be a ring closed PI structure with the fourth segment being a more flexible PAA repeat unit. However, the presumption that

* To whom correspondence should be addressed.
† Current address: Film Technology Center, 3M Center Building 236-GA-03, St. Paul, MN 55144-1000.
• Abstract published in *Advance ACS Abstracts,* October 15, 1993.

0024-9297/93/2226-6557$04.00/0

an amic acid unit is periodically spaced at every fourth chemical repeat seems unlikely when considering that imidization of PAA chains should proceed randomly along the chain backbone. The limited selected-area electron diffraction (SAED) data presented and the lack of HREM images within the lamellar domains left unanswered questions about molecular organization and the predominant defects that form in crystalline PMDA–ODA.

Detailed studies of dislocation defects in lamellar polymer crystals have been limited by the resolution of characterization techniques typically employed. The growth of terraces a crystal edges are usually associated with the presence of screw dislocations.[9] Polyethylene crystals have been found to have screw dislocations with the Burgers vectors approximately equal to the lamellar thickness.[10] Scanning tunneling microscopy (STM) images of poly(ethylene) single crystals[11] have shown morphologies consistent with growth around screw dislocations followed by chain slip during deposition onto the substrate. Since semiflexible PMDA–ODA molecules form lamellar crystals from dilute solution, similar screw dislocation mediated growth might be expected.

By using low electron doses, we found that HREM imaging of the molecular structure of these crystals could be achieved without significant damage to the polymer. This technique allowed local characterization of defects in the crystalline packing of the PMDA–ODA molecules. We also examined the morphology of the PMDA–ODA crystals with atomic force microscopy (AFM).[12] The AFM provided high resolution information about surface structure which proved to compliment the information obtained by conventional TEM methods.

The unit cell for PMDA–ODA is monoclinic (pseudoorthorhombic)[5,6] ($P2/c$) with unit cell dimensions of a = 0.631, b = 0.402, and c (chain axis) = 3.258 nm. Fiber diffraction patterns indicate that $\alpha = \beta = 90°$. However, it has been argued that the crystallographic angle γ may vary as much as 10° from 90°.[13] Before this study conclusive information about fluctuations in γ had not yet been obtained.

II. Experimental Section

PMDA–ODA poly(amic acid) of 1.23 dL/g intrinsic viscosity was provided by the DuPont Co., Wilmington, DE, in a concentrated solution of 15% by weight in 1-methyl-2-pyrrolidinone (NMP). The weight average molecular weight (M_w) was estimated to be 31 000 from the Mark–Houwink relation ($[\eta] = 0.058M_w^{0.74}$) reported by Cotts.[14]

A 1.4% by weight solution of the PMDA–ODA PAA was prepared by dilution in NMP, used as received. After heating the solution to 160 °C in a pure nitrogen atmosphere the solution became turbid due to crystallization after approximately 1 h.[8] The sample was held at 160 °C for a total of 130 min. After cooling to room temperature, droplets of the crystalline suspension were transferred onto holey-carbon coated copper TEM support grids from a glass capillary tube.

The extent of imidization in the samples was examined by Fourier transform infrared spectroscopy (FTIR) using a Mattson instruments Galaxy Series 3000 FTIR operating in the diffuse reflectance mode and a SpectraTech FTIR microscope operating in tranmission mode. The integrated areas of the 725-cm^{-1} imide band and 1225-cm^{-1} diphenyl ether stretch bands were compared to standard samples of fully imidized films provided by DuPont and prepared in our laboratory. This analysis indicated that the extent of reaction of the lamellar crystals was greater than 95%. AFM samples were prepared by atomization of the crystalline suspension onto (100) silicon substrates. Silicon wafers were sectioned into 2- × 2-cm squares by diamond scribing followed by thoroughly wiping the substrates clean with acetone and laboratory tissue. A 5-mL charge of the lamellar crystal solution was placed in a nebulizer (Ted Pella, Inc.) and sprayed onto the silicon substrates. Five to ten sprays provided a high density of droplets with a significant concentration of crystals. The dynamics of the atomization process promoted individual crystals to adhere to the substrate independently without associated liquid. This allowed force imaging without artifacts or perturbations resulting from contact of the tip with excess unconverted PAA solution or residual solvent covering and surrounding the crystals.

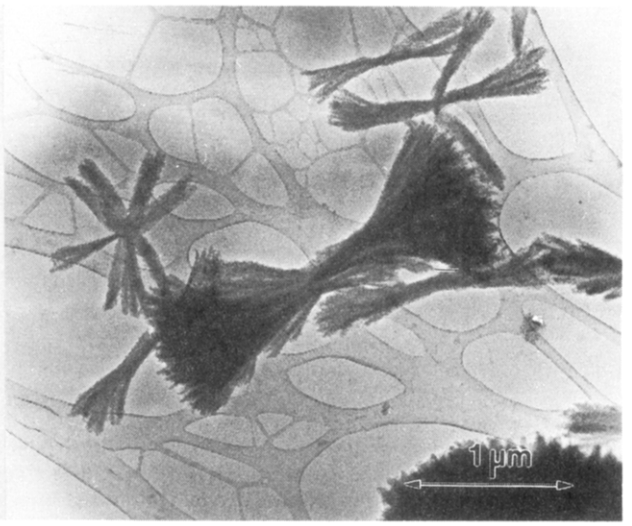

Figure 2. Bright field micrograph of PMDA–ODA single crystals on a holey carbon substrate.

The samples were examined with a JEOL 4000 EX transmission electron microscope at an accelerating voltage of 400 kV using a minimum dose system (MDS) and beam blanking device. Low dose HREM was used to image the strong 1.6-nm (002) planar spacings corresponding to the PMDA–ODA chemical repeat unit.[5] Also, lattice fringes of the lateral ((100) and (010)) 0.4- and 0.6-nm packing directions were obtained using this method. Magnifications ranging from 80- to 150k× were chosen for high resolution work.

Specific experimental procedures for low dose HREM imaging have been discussed elsewhere.[15,16] In particular, it has been shown[17,18] that maximizing the phase contrast of crystalline spacings of size d can be obtained by using an underfocus condition determined by $d^2/2\lambda$. This gives an optimum underfocus of 800 nm for obtaining the 1.6-nm (002) fringes at 400 kV (λ = 1.64 pm).

The total end point dose (TEPD) for disappearance of the crystalline reflections in selected area diffraction (SAED) patterns from the lamellar crystals was determined to be 0.22 ± 0.07 C/cm^2. This value is consistent with the trend relating beam damage in polymers to thermal stability.[19] During HREM imaging the samples were exposed to less than one-third of this dose to avoid damaging the crystal structure.

Lattice fringe spacings and SAED patterns were calibrated by evaporating gold onto the sample. HREM images were calibrated using a He–Ne laser optical bench with images of turbostratic graphite (0.34 nm). Negatives or high contrast prints were digitized with a CCD camera and Scion image video 1000 broad. The images were analyzed with the FFT Image (Version 1.35)[20] software.

Morphological and topographical features of the PMDA–ODA lamellar crystals were obtained used a Digital Instruments Nanoscope III AFM with the A, D, and J force heads. The crystals were examined in air on silicon substrates using silicon nitride and single crystal silicon tips. Software features allow quantitative estimates of height variations from the sample to the substrate.

HREM images were generated from the MacTempas simulations software, available from the National HREM Facility at Lawrence Berkeley Laboratory. Molecular simulations of the PMDA–ODA crystal structure, energy, diffraction patterns, and high resolution images were generated with Cerius and PolyGraf, both commercially available from Molecular Simulations, Inc. Two-chain unit cells were used to explore the influence of local variations in molecular packing on crystal energy by doubling the length of the unit cell in either the a or b axis direction and

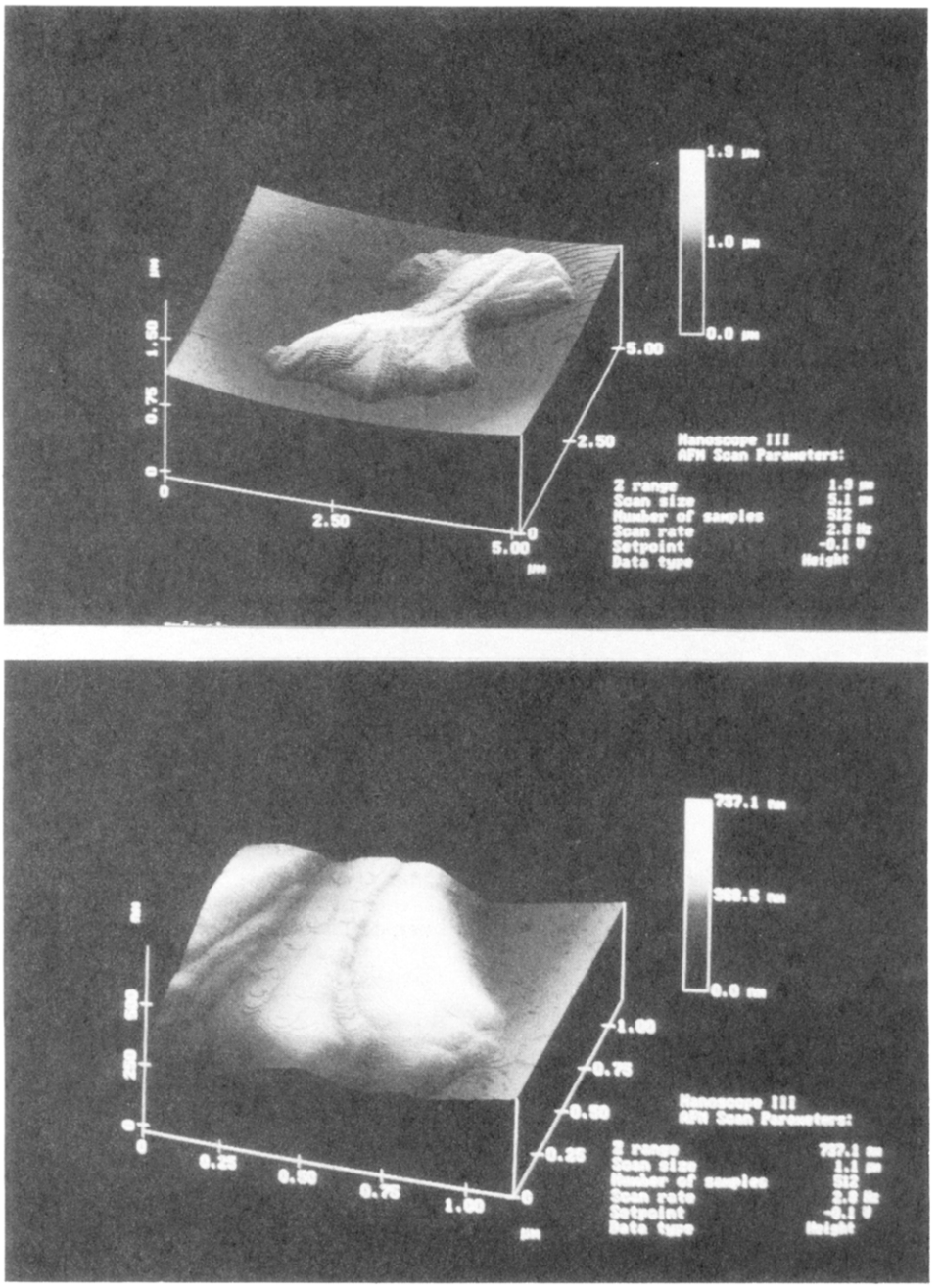

Figure 3. (a, Top) Atomic force microscope image of an isolated spherulite of PMDA–ODA grown from solution. (b, Bottom) Detail of crystal edge revealing steps and terraces of approximately 10 nm in height consistent with the morphology seen in the TEM.

redefining the unit cell parameters accordingly. Copies of our structural model computer files are available upon request.

III. Results and Discussion

A. General Observations. TEM studies of the PMDA–ODA single crystals revealed lamellar crystals ranging in size from 0.5 to 5 μm. Figure 2 shows a typical distribution of sizes and morphologies of the PMDA–ODA lamellar crystals. Figure 3a is an AFM scan showing a 4-μm-long lamellar crystal. Many of the PMDA–ODA crystals grown from solution had this distinctive bow tie morphology consistent with a spherulite nucleus. Close examination of this particular crystal showed that it consisted of independent bundles of lamellae. These bundles had an average width of about 250 nm. The fact that the maximum height and lateral splay of the lamellar crystal occurred at the two ends of the structure provided evidence that the crystal growth direction was parallel to the bow tie axis with the thickness increasing as growth occurs away from the center. Height calculations revealed a maximum thickness located at the center of the splayed regions and dependent on the overall size of the crystal. Generally, the thickness at the outer perimeter of PMDA–ODA lamellar crystals ranged from 5 to 15 nm. Figure 3b is an AFM micrograph of the lamellar crystal viewed down the growth direction. Close examination at the end of the crystal revealed steps or terraces or 10 nm in height, familiar features of chain folded polymer lamellar crystals.[12,21,22]

The [010] direction was the primary growth habit of the PMDA–ODA lamellar crytals. A common feature in TEM were collections of two or more crystals with a "crossed" texture. Figure 4 shows such a PMDA–ODA bicrystal morphology with each crystal oriented roughly normal to the other. The crystal running from top to bottom of the micrograph is oriented with the [100] direction parallel to the electron beam. The 1.6-nm (002) fringes are visible in the region near the crystal's edge. SAED diffraction of the horizontal crystal revealed that the [001] (chain) direction was normal to the substrate.

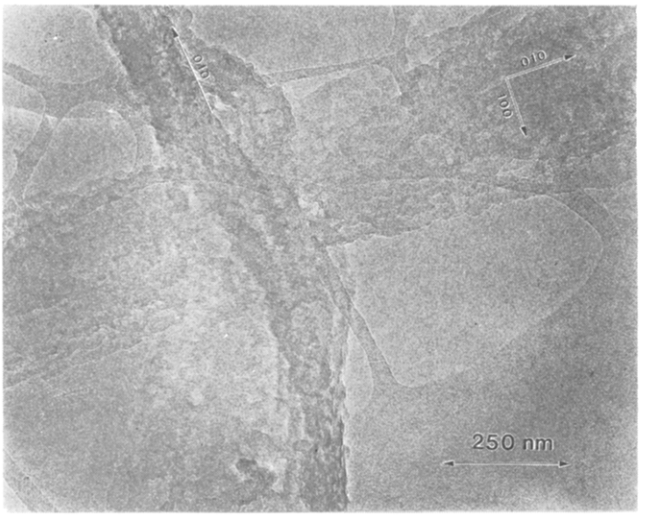

Figure 4. Center of a PMDA–ODA "crossed" crystal texture indicating two crystals oriented nominally perpendicular to one another to make a bicrystal. Both crystals have the [010] direction as the fast growth axis.

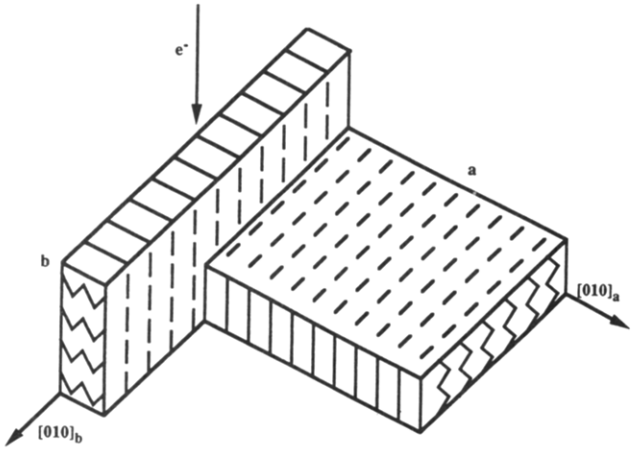

Figure 5. Schematic diagram of the "crossed" bicrystal texture in Figure 4. The electron beam (e^-) is parallel to the [001] (chain) direction for a crystal **a** and the [100] direction for crystal **b**.

A schematic representation of the bicrystal morphology is given in Figure 5.

Intercrossing growth in polymer crystals has been shown to occur in other semicrystalline polymers such as polyethylene and polypropylene.[22–27] Khoury[22] has shown independent growth incident resulting in nucleation of another lamellar structure from the parent of lamellar polypropylene crystals. Growth of the new segment was found to be transverse to the parent crystal direction and established epitaxy between crystals. This mechanism of branching via epitaxial overgrowth formation was termed "quadrite" since the new crystal grows normal to the parent forming a bicrystal.

B. Observations from the Side ([100] Zone). From HREM images of the 1.6-nm spacings down the [100] zone individual lamellae of consistent thickness could be distinguished. Typically, the lamellea were on the order of 10 nm, as is shown in Figures 6 and 7. The PMDA–ODA molecules are oriented perpendicular to the fringe direction. The lamellar thickness corresponds to six 1.6-nm (002) repeat units along the chain backbone. The high contrast and extended lateral size of the (002) fringes within

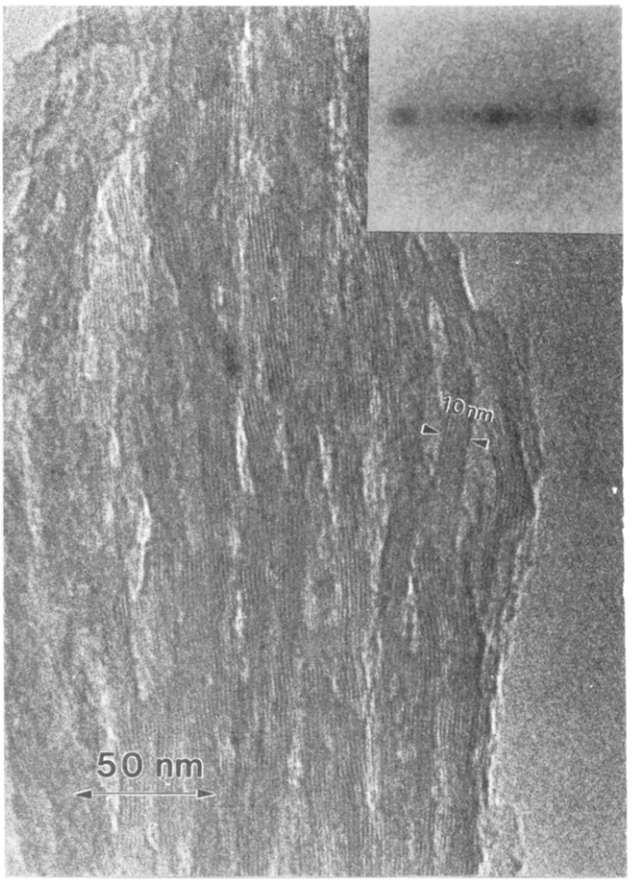

Figure 6. HREM image of PMDA–ODA crystal lamellae. The predominant spacing in this image is 1.6 nm (002) which is perpendicular to the chain direction. The inset shows the digital FFT of the image from which both the (002) spacing and average lamellar repeat distance can be determined.

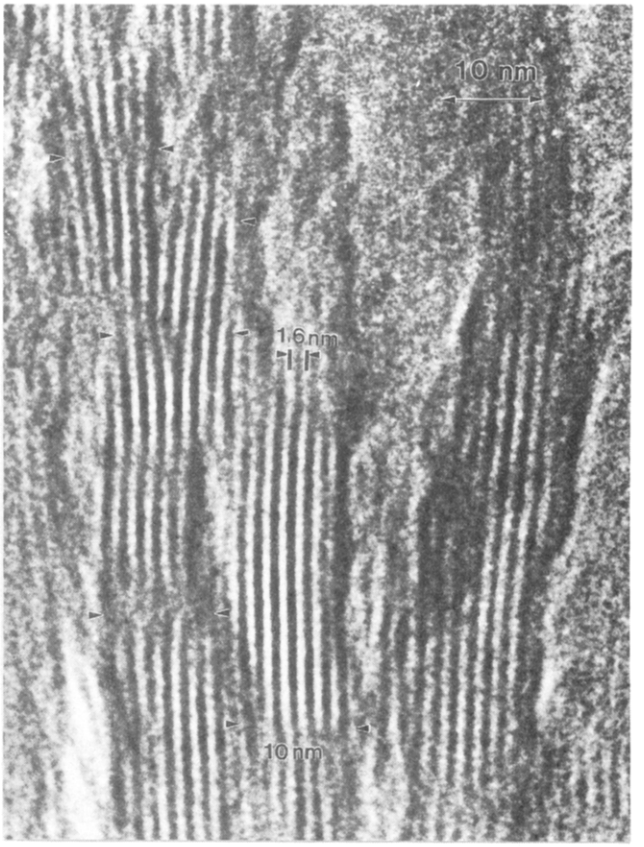

Figure 7. Higher magnification view showing high resolution detail within individual PMDA–ODA lamellae. Evidence for screw dislocations can be identified (arrows).

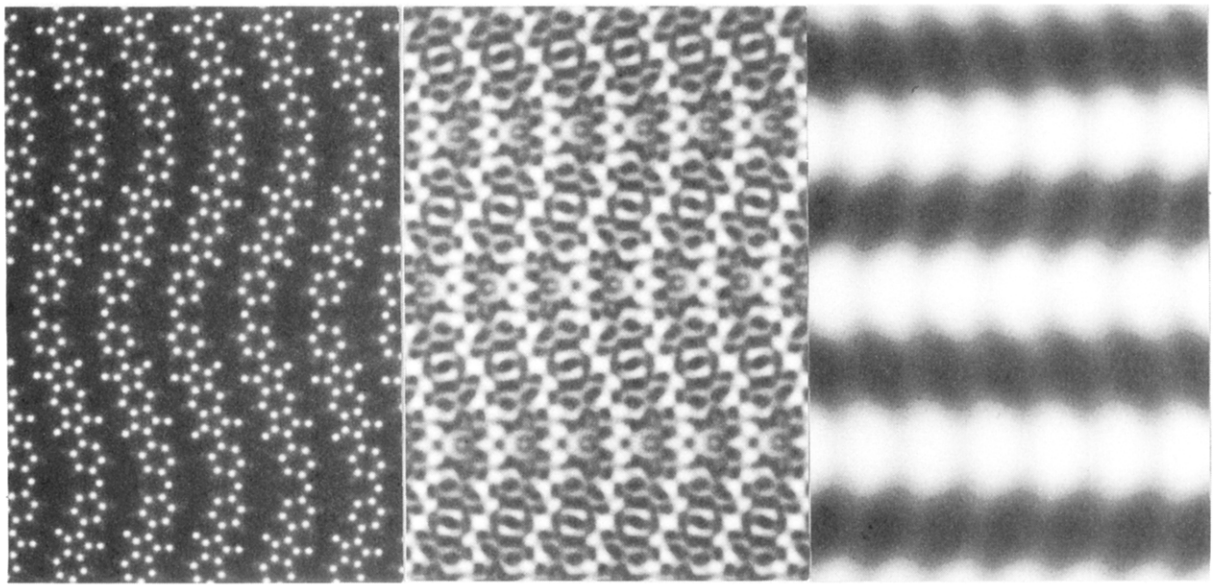

Figure 8. (a, Left) projected electron potential of crystalline PMDA–ODA in the [010] direction showing the zigzag conformation of the molecule. (b, Middle) simulated HREM image of PMDA–ODA at Scherzer defocus (C_s = 0.7 mm, E_o = 400 kV, defocus spread = 8 nm, beam divergence = 0.5 mrad, crystal thickness = 10 nm). (c, Right) simulated HREM image of PMDA–ODA at an underfocus of −800 nm showing the strong 1.6-nm (002) spacings, as seen experimentally (Figures 6 and 7). In the theoretical simulations the white fringe of the image corresponds to the location of the diphenol ether link between alternating units of the PMDA–ODA molecule.

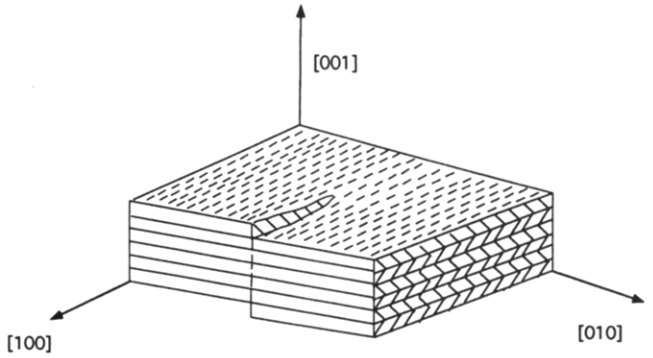

Figure 9. Schematic of a screw dislocation in PMDA–ODA consistent with the HREM image contrast observed in Figure 7 and molecular simulations which suggest that slip should occur primarily on the (010) crystal faces due to the "zig" and "zag" of the molecules on (100).

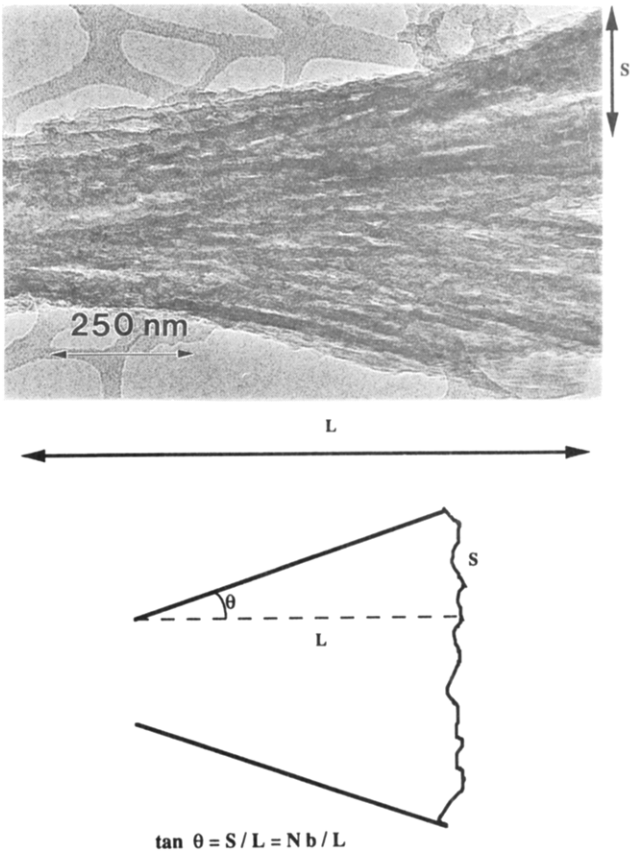

Figure 10. Experimental HREM image and schematic diagram of the lateral splay induced by screw dislocations in PMDA–ODA crystals. The increase of width (S) over a given length (L) is related to the number of dislocations (N) times their Burger's vector (b). Hence, the tangent of the divergence angle (θ) is Nb/L.

the lamellae are remarkable and provide for unambiguous evidence of the regularity of axial registry between neighboring molecules in crystalline PMDA–ODA. The 1.6-nm (002) fringes of Figures 6 and 7 were found experimentally using the $d^2/2\lambda$ defocus condition for maximum phase contrast of these lattice spacings. This result was confirmed with the MacTempas HREM image simulation software. The atomic coordinates and crystal symmetry were obtained by minimizing a PMDA–ODA moiety using triply periodic boundary conditions and the Dreiding II force field in PolyGraf. The minimization was carried out using orthorhombic symmetry and the unit cell dimensions provided by Kazarayan et al.[5] The microscope parameters used correspond to those of the JEOL 4000 EX: C_x = 0.7 mm, E_o = 400 kV, defocus spread = 8.0 nm, divergence angle = 0.5 mrad. In the simulation, as in the experiment, we used no mechanical aperture. This has the disadvantage of reducing contrast somewhat but the significant advantage of limiting resolution only by the damping nature of the transfer function. It also makes it easier to adjust to the objective lens astigmatism, since this setting is sensitive to the precise position of the aperture.

Figure 8a shows the projected electron potential of the stable PMDA–ODA crystal lattice from the minimization; Figure 8b shows simulated image at the optimum Scherzer defocus condition of −33.7 nm, and Figure 8c the maximum contrast defocus (−800 nm) for the (002) repeat spacing. Both of these images were calculated for a crystal thickness of 10 nm. The latter image (8c) shows that at the focus used in our experiment and for a 10-nm-thick sample the bright regions in the HREM image should be associated

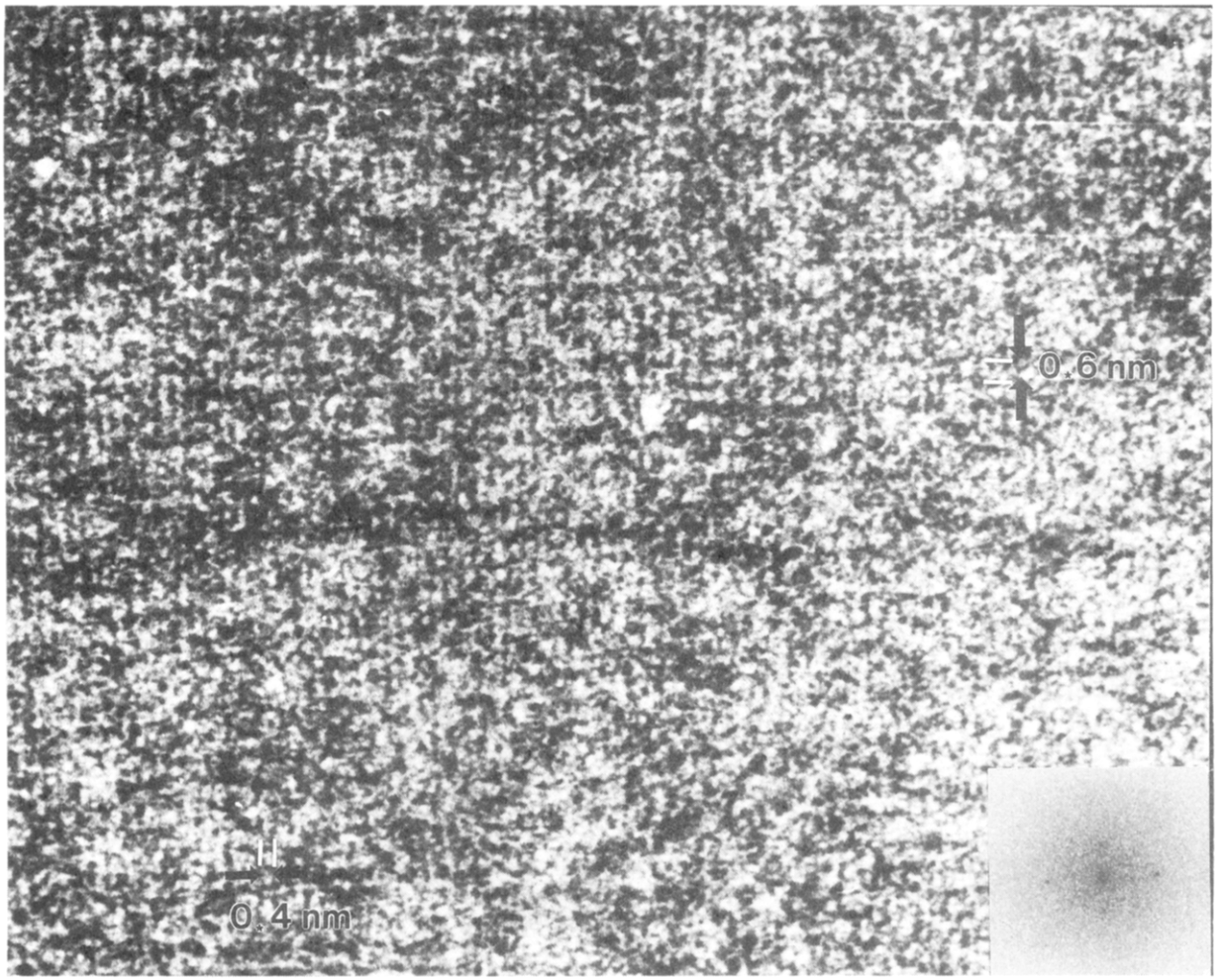

Figure 11. HREM image down the chain axis (in the [001] zone) of PMDA–ODA showing the 0.6-nm (100) and 0.4-nm (010) spacings. A digital FFT is inset.

with the ether linkage of the ODA unit.

Lebedev[8] suggested that the consistent lamellar thickness of PMDA–ODA could be the result of folding at an unconverted amic acid linkage at every fourth repeat. Chain ends may also be contributing to the density drop-off at the fold surface where vacancies result from termination.[28] An alternative scenario which we favor simply involves local bending of the PMDA–ODA molecule at either the diphenol ether bond or the imide nitrogen. Lovinger et al.[29] and Hudson et al.[30] observed similar lamellar crystals in crystallized poly(aryl–ether–ether–ketone) (PEEK). This semicrystalline polymer also has diphenol–ether bonds along its backbone which apparently act as sites for chain folding.

While experimental evidence consistent with large deformation of covalent bonds at room temperature is interesting, scrutiny of the literature reveals that it is not without precedent. Local HREM observations of the deformation within kink bands of oriented rigid-rod polymer fibers at molecular resolution has also provided support for covalent bond bending at ambient temperature.[31] The fact that molecules such as cyclopropane even exist provides further support for the resiliency of the covalent bond to large angle deformations. The ability to induce dramatic changes in the conformation and energetic state of the molecule by appropriate processing conditions (such as crystallization or mechanical deformation) may provide an interesting new research focus for solid-state polymer physics. Since such events might occur only occasionally throughout the material, the analysis of these phenomena via local high resolution structural characterization techniques is an important development.

Distinctive defects with a Burgers vector of 1.6 nm [002] (extra fringe) can be identified in Figure 7. Here the contrast is consistent with a screw dislocation that has a Burger vector which is only half of the true (3.2 nm) repeat of the molecule (Figure 9). This differs significantly from other polymer lamellar crystals (i.e., polyethylene) where the Burgers vector of the screw dislocation is on the order of the 10-nm lamellar thickness.[11] Also, note that there is evidence for a screw dislocation relatively often; in fact evidence for such a defect is seen about once every 10 nm along the growth direction.

The lateral growth of the PMDA–ODA crystals can be directly associated with these screw dislocations. We estimated the number of defects required to produce the splay experimentally observed in PMDA–ODA lamellar single crystals. This analysis accounted for the total number of defects with a 1.6-nm Burgers vector leading to the increased lateral displacement as growth occurs along the lamellar direction away from the nucleation site (Figure 10). The geometric dislocation density is calculated using the relationship[32] $\tan \theta = Nb/L$. The dislocation density per length (L) of the lamellar crystal was found by calculation of the tangent of the angle formed between the splay length (S) (lateral gradient) and L. Figure 10 shows a spherulite with splay deformation consistent with a b = 1.6 nm screw dislocation located every 9 nm along the lamellar crystals. This result corresponds with the 10-nm value estimated from the direct imaging of the defects by HREM (Figure 7).

To reveal more insight about our proposed dislocation model, we examined the theoretical crystal energy of PMDA–ODA as a function of anticipated distortions

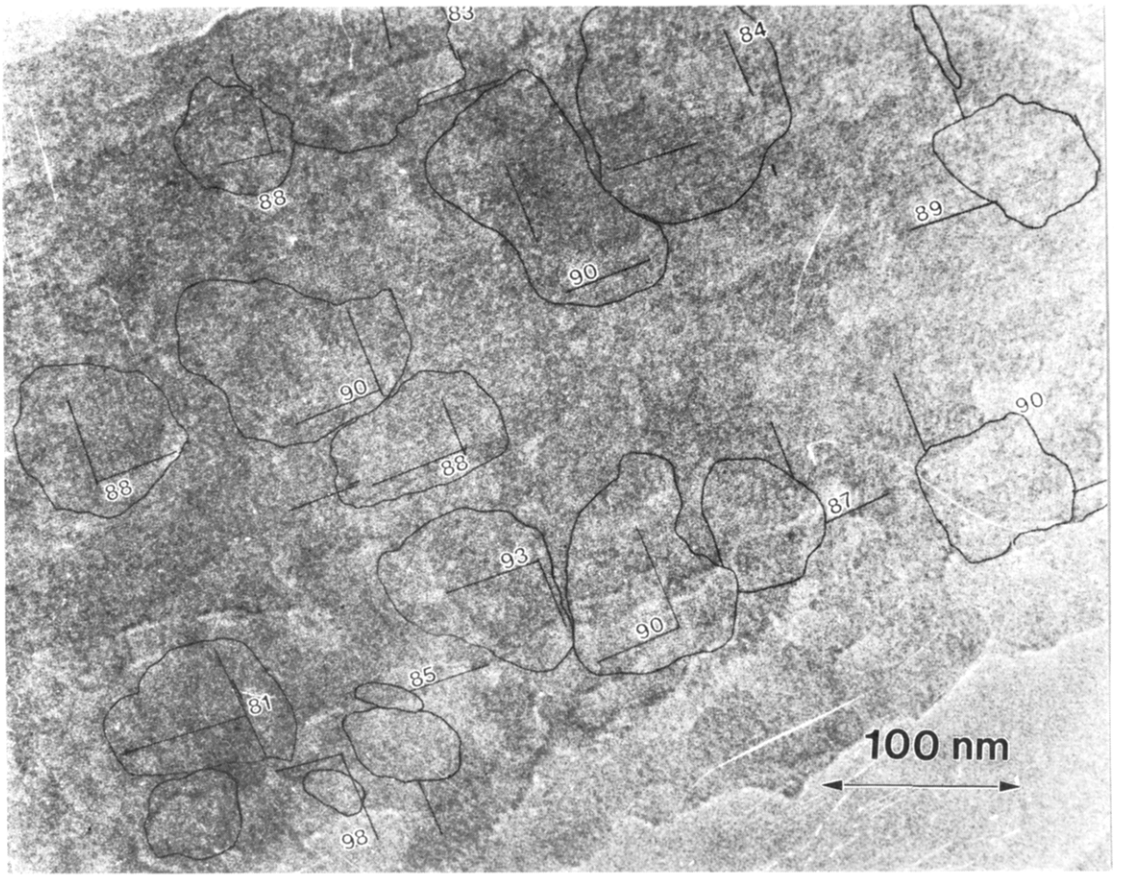

Figure 12. HREM image showing domains in which the crystallographic angle γ is locally constant. The local fluctuations in γ from domain to domain are shown on the figure.

within the unit cell. Using Cerius[31] the theoretical crystal energy of PMDA–ODA in a two-chain orthorhombic unit cell was determined as a function of the translation of one molecule relative to another along the chain axis. Relative translations in the [001] direction across the (100) planes were examined by expanding the unit cell once in the a direction and across the (010) by expanding the unit cell in the b direction. The distortion was introduced by moving the second chain along [001] with respect to the first. The predicted variations in energy on the (010) face are 680 kcal/mol, with 10 local minima evident. However, performing the same calculation with the (100) faces as the contact surface shows that translation of the molecule along [001] would lead to unrealistically high energy spikes due to improper superposition of the "zig" and "zag" of the 2-fold PMDA–ODA helix. We therefore anticipate that such axial misregistry across the (100) face is unlikely without a significant expansion of the distance between PMDA–ODA chain backbones.

Digitizing the images from the HREM micrographs in Figures 6 and 7 and calculating the digital transform using FFT Image[20] makes it possible to estimate the lamellar thickness and (002) lattice spacings. The dimensions so determined were 1.53 ± 0.1 and 10.2 ± 0.5 nm for the (002) lattice spacing and the lamellar thickness, respectively. The value of the (002) lattice spacing calculated from laser optical diffractograms was found to be 1.55 ± 0.05 nm. The fact that these (002) spacings are less than the 1.62 nm estimated from fiber WAXS is consistent with the results of Factor et al.[4] who found that the molecules in the bulk of PMDA–ODA films had reduced (002) spacings along the chain direction. These results suggest that there may be out of plane rotation of the molecule at the diphenol–ether bond or bending at the imide nitrogen, reducing the projection of the repeat unit along the chain axis.

C. Observations from the Top ([001] Zone). Enlarged 0.6 and 0.4 lattice fringes corresponding to the (100) and (010) planes are shown in Figure 11. The parameters of the orthorhombic cell were estimated from digital FFTs to be $a = 0.65 \pm 0.05$ nm and $b = 0.41 \pm 0.05$ nm. The lateral size of these crystalline domains were quite large (50–100 nm). The domains were also quite perfect, with little or no evidence for dislocations with Burgers vectors in the $\langle hk0 \rangle$ directions.

Occasionally, both the (100) and (101) spots could be identified in digital FFTs of the HREM images. The (101) spot is particularly intense in PMDA–ODA fiber and powder X-ray patterns due to the slight inclination of the poly(imide) chains to the fiber axis (Figure 8). Because of the large d spacing in the chain direction (3.2 nm), the angle between the (100) and (101) planes is only 10°.

Our HREM experiments revealed apparent fluctuations in the crystallographic angle (γ) between the 0.6- (100) and 0.4-nm (010) planes. Figure 12 shows an enlarged region of a crystal with the electron beam oriented parallel to the [001] chain axis. The micrograph shows several regions where the angle (γ) between these fringes is not the 90° expected for an orthorhombic unit cell.[5] Instead, the fringes indicate that γ fluctuates from 81 to 99° in different regions of the crystal. A frequency plot of the angular distortion $|90 - \gamma|$ is given in Figure 13. This graph was constructed from measuring the angles of lateral packing cross fringes from several high contrast glossy HREM prints. The typical fluctuations are ±5° although occasional observations up to 9° are also found.

Once the crystallographic angle γ fluctuates away from 90°, it is also possible to consider variations in the angle θ between the plane of the PMDA–ODA molecule and the a axis. Figure 15 shows a plot of the theoretical crystal energy as a function of γ and θ. The contours are drawn at intervals of 2 kcal/mol. Note the valley indicating that

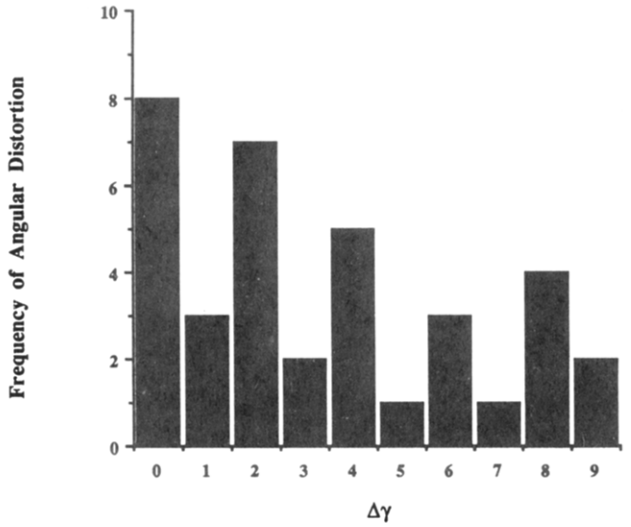

Figure 13. Frequency plot of the distortions of the crystallographic angle γ as observed in the [001] HREM lattice images.

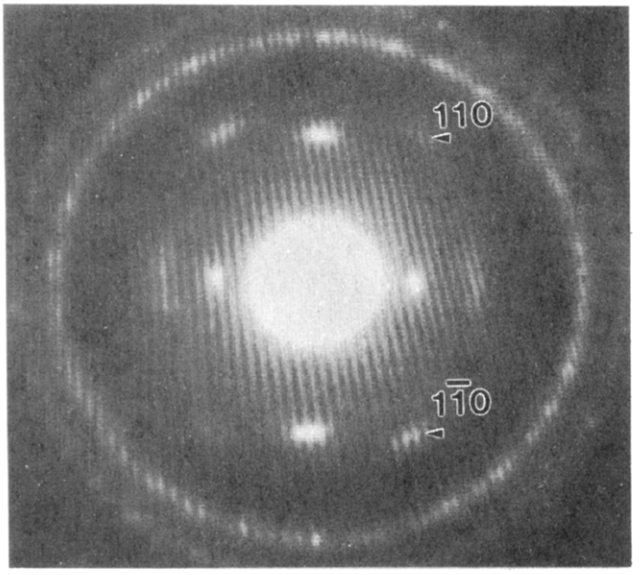

Figure 14. Experimental SAED showing a difference in the relative intensity of the (110) and (1, −1, 0) spacings. The measured difference in relative intensity corresponds to a fluctuation of 2° in the angle γ.

there is a considerable region of conformational space available to PMDA–ODA. The plot suggests that any fluctuations in γ should be accompanied by a corresponding variation in θ to minimize the energy.

If the monoclinic angle γ (and θ) deviate from 90° (0° for θ) then there should be a corresponding change in the relative intensity and position of the (110) and (1, −1, 0) reflections. The intensity of a typical PMDA–ODA (video digitized) SAED pattern down the [100] zone of these lamellar crystals is shown in Figure 14. The differences in the relative intensity of the (110) and (1, −1, 0) reflections are consistent with fluctuations in either γ or θ, while the lack of higher order reflections can only be explained by fluctuations in γ. By measuring the relative intensity of the (110) and (1, −1, 0) reflections the deviation in γ consistent with these data can be estimated. The intensity of the (110) reflection was found to be 3 times as intense as the (1, −1, 0) reflection in Figure 14. Calculations using Cerius predict this change in relative intensity should occur when γ is shifted by 2°.

The observation that the crystallographic angle is locally constant indicates that PMDA–ODA crystals are composed of domains separated from one another by lateral

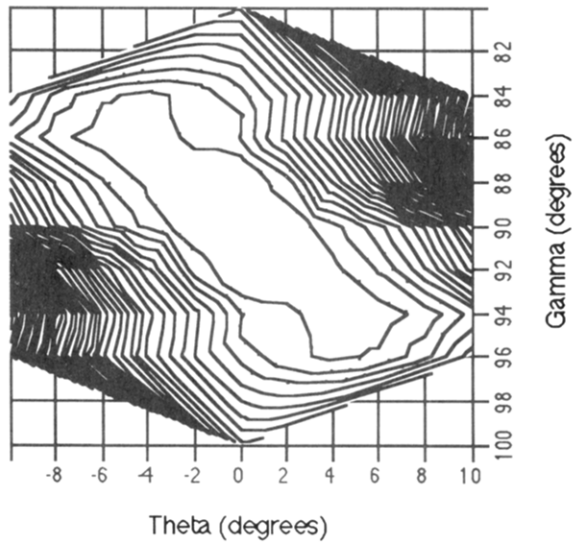

Figure 15. Contour plot of the theoretical crystal energy as a function of the crystallographic angle γ and the molecular setting angle θ. The contours are drawn at energy increments of 2 kcal/mol. There is a valley in the energy surface indicating that simultaneous variations of up to 5° in γ and θ have little influence on the crystal energy, as suggested by experiment.

chain invariant (LCI) grain boundaries.[33] The chains on either side of the boundary are oriented in the same direction, but there are local fluctuations in the value of γ. Future work will be required to reveal the detailed structure of and possible influence of these boundaries on macroscopic properties.

Our results unambiguously confirm that PMDA–ODA can exhibit well-defined crystalline domains. High degrees of order have also been found for PMDA–ODA during imidization under elevated pressure.[34] These observations point out the need to carefully examine the specific processing route used to prepare poly(imides) in order to understand and predict microstructure. For example, the relationship between the conversion to imide, loss of solvent, and extent of crystallinity has been described in terms of a ternary phase-stability diagram.[35] This scheme makes it possible to track the structural evolution during the simultaneous loss of solvent and imidization during processing.

IV. Conclusions

Solution grown lamellar single crystals permit an analysis of the local order and defect structure in PMDA–ODA. The lamellar crystals consistently displayed a uniform 10-nm thickness when imaged from an edge-on orientation, suggesting that this PI has the ability to chain fold. HREM images of the 1.6-nm (002), 0.6-nm (100), and 0.4-nm (010) crystalline planes have all been obtained. Evidence for screw dislocations with a Burgers vector of [001] and magnitude of $c/2$ (1.6 nm) have been found. The lateral splay of the PMDA–ODA lamellae is associated with these defects. Local fluctuations in the packing geometry (±9° in the crystallographic angle γ) have also been observed.

Acknowledgment. This work was supported by DuPont, the University of Michigan, and the National Science Foundation (NYI program). The authors also thank Dr. James Edman, Dr. Larry Berger, and Dr. Kenn Gardner of DuPont for supplying materials and technical assistance. The facilities and staff support of the University of Michigan Electron Microbeam Analysis Laboratory

(EMAL) are gratefully acknowledged. Significant efforts by Patricia Wilson in helping to obtain the low dose HREM images are also recognized.

References and Notes

(1) Russell, T. P. *J. Polym. Sci., Part B: Polym. Phys.* **1984**, *22*, 1105.
(2) Russell, T. P.; Gugger, H.; Swalen, J. D. *J. Polym. Sci., Part B: Polym. Phys.* **1983**, *21*, 1745.
(3) Takahashi, N.; Yoon, D. Y.; Parrish, W. *Macromolecules* **1984**, *17*, 2583.
(4) Factor, B. J.; Russell, T. P.; Toney, M. F. *Phys. Rev. Lett.* **1991**, *66*, 1181.
(5) Kazarayan, L. G.; Tsvankin, D. Y.; Ginzburg, B. M.; Tuichiev, S.; Korzhavin, L. N.; Frenkel, S. N. *Vysokomol. Soedin.* **1972**, *A14*, 1199.
(6) Freilich, S. C.; Gardner, K. H. In *Polyimides: Materials, Chemistry, and Characterization*; Feger, C., Khojasteh, M. M., McGrath, J. E., Eds.; Elsevier Science Publishers, B.V.: Amsterdam, 1989; p 513.
(7) Russell, T. P.; Brown, H. R.; Grubb, D. T. *J. Polym. Sci., Part B: Polym. Phys.* **1987**, *25*, 1129.
(8) Lebedev, G. A. *Vysokomol. Soedin.* **1975**, *A17*, 1164.
(9) Keller, A. *Kolloid Z. Z. Polym.* **1967**, *219*, 118.
(10) Shultz, J.; *Polymer Materials Science*; Amundson, N. R., Ed.; Prentice-Hall, Inc.: Englewood Cliffs, NJ, 1967.
(11) Piner, R.; Reifenberg, R.; Martin, D. C.; Thomas, E. L.; Apkarian, R. P. *J. Polym. Sci., Part C: Polym. Lett.* **1990**, *28*, 399.
(12) Patil, R.; Kim, S.-J.; Smith, E.; Reneker, D. H.; Weisenhorn, A. L. *Polym. Commun.* **1990**, *31*, 455.
(13) Conte, G.; D'Ilario, L.; Pavel, N. V. *J. Polym. Sci., Part B: Polym. Phys.* **1976**, *14*, 1553.
(14) Cotts, P. M. In *Polyimides: Synthesis, Characterization and Applications*; Mittal, K. L., Ed.; Plenum Press: New York, 1984; p 223.
(15) Tsuji, M. In *Comprehensive Polymer Science*; Allen, G., Bevington, J. C., Eds.; Price, C. Colin, Series Ed.; Pergamon Press: Oxford, U.K., 1989; Vol. 1.
(16) Voight-Martin, I. G.; Krug, H.; Van Dyck, D. *J. Phys. Fr.* **1990**, *51*, 2347.
(17) Martin, D. C.; Berger, L. L.; Gardner, K. H. *Macromolecules* **1991**, *24*, 3921.
(18) Pradere, P.; Thomas, E. L. *Macromolecules* **1990**, *23*, 4954.
(19) Kumar, S.; Adams, W. W. *Polymer* **1990**, *31*, 15.
(20) 1.35 FFT Image software by W. Rasband, National Institutes of Health, Research Science Branch, NIMH; modified by the Electron Microbeam Analysis Laboratory (EMAL) at the University of Michigan.
(21) Reneker, D. H.; Geil, P. H. *J. Appl. Phys.* **1960**, *31*, 1916.
(22) Khoury, F. *J. Res. Natl. Bur. Stand.* **1960**, *A70*, 29.
(23) Padden, F. J.; Keith, H. D. *J. Appl. Phys.* **1973**, *44*, 1217.
(24) Lotz, B.; Graff, S.; Straupe, C.; Wittman, J. C. *Polymer* **1991**, *22*, 2902.
(25) Lotz, B.; Wittman, J. C. *J. Polym. Sci., Part B: Polym. Phys.* **1986**, *24*, 1541.
(26) Lotz, B.; Lovinger, A. J.; Cais, R. E. *Macromolecules* **1988**, *21*, 2375.
(27) Padden, F. J.; Keith, H. D. *J. Appl. Phys.* **1966**, *37*, 4013.
(28) Keith, H. D.; Passaglia, E. *J. Res. Natl. Bur. Stand.* **1964**, *A68*, 513.
(29) Lovinger, A. J.; Hudson, S. D.; Davis, D. D. *Macromolecules* **1992**, *25*, 1752.
(30) Hudson, S. D.; Davis, D. D.; Lovinger, A. J. *Macromolecules* **1992**, *25*, 1759.
(31) Martin, D. C.; Thomas, E. L. *J. Mater. Sci.* **1991**, *26*, 5171.
(32) Klemen, M. *Points, Line, and Walls: In Liquid Crystals, Magnetic Systems, and Various Ordered Media*; J. Wiley: Chichester, New York, 1983.
(33) Martin, D. C.; Thomas, E. L. *Philos. Mag. A* **1991**, *64* (4), 903.
(34) Jennings, R. Ph.D. Dissertation, University of Massachusetts at Amherst, 1993.
(35) Ojeda, J. R.; Mobley, J.; Martin, D. *J. Polym. Sci., Polym. Phys. Ed.*, submitted for publication.